

The $\mathcal{PP}2\mathcal{PP}$ Experiment at RHIC*

J. CHWASTOWSKI

Henryk Niewodniczański Institute of Nuclear Physics,
Cracow

(for The $\mathcal{PP}2\mathcal{PP}$ Collaboration [1])

The $\mathcal{PP}2\mathcal{PP}$ experiment is devoted to the proton – proton elastic scattering measurements at the Relativistic Heavy Ion Collider (RHIC) at the centre-of-mass energies $50 \leq \sqrt{s} \leq 500$ GeV and the four-momentum transfer $0.0004 \leq |t| \leq 1.3$ GeV². The option of polarized proton beams offers a unique possibility to investigate the spin dependence of the proton elastic scattering in a systematic way. The energy dependence of the total and elastic cross section, the ratio of the real to the imaginary part of the forward scattering amplitude, and the nuclear slope parameter will be studied. In the medium $|t|$ region ($|t| \leq 1.3$ GeV²) the energy dependence of the dip structure in the elastic differential cross section will be measured. With polarized beams the measurement of spin dependent observables: the difference of the total cross sections as function of the of initial transverse spin states, the analyzing power and the double spin asymmetries will be used to map the s and t dependence of the proton helicity amplitudes.

PACS numbers: PACS 13.75.C, 13.85, 13.85.D

1. Introduction

The elastic channel contributes about 20% to the total cross section. This, coupled with the necessity of explaining diffraction in terms of QCD, makes the nucleon – nucleon elastic scattering a very attractive tool for the exchange mechanism investigation. So far, the elastic proton – proton scattering was studied up to the highest ISR energies ($\sqrt{s} = 62$ GeV) while for $\bar{p}p$ the measurements reached $\sqrt{s} = 1.8$ TeV. The ISR data confirmed earlier prediction [2, 3] of the total cross section rise with energy. Also Pomeranchuk's prediction [4] on the asymptotic behaviour of the total cross

* Presented at Cracow Epiphany Conference on Quarks and Gluons, 3 – 6 January, Cracow, Poland

sections for pp and $\bar{p}p$ scattering was extensively tested. Summary of elastic scattering measurements and phenomenological models can be found in [5].

With advent of the Relativistic Heavy Ion Collider (RHIC) at Brookhaven National Laboratory a new energy domain opens for a study of the proton - proton scattering. The accelerator is capable of delivering proton beams [6] polarized up to 70% with luminosities reaching $\mathcal{L} = 10^{31} \text{cm}^{-2} \text{s}^{-1}$. This offers a unique opportunity for a systematic study of the spin dependent and spin independent elastic scattering in a new, mostly unexplored centre-of-mass energy range of $50 \leq \sqrt{s} \leq 500$ GeV and for the four-momentum transfer $0.0004 \leq |t| \leq 1.3$ GeV² [7].

The colliding of polarized beams allows for the measurement of the proton helicity structure in wide range of $|t|$ and energy within a single experiment. The polarization studies will shed a light onto emerging new picture of diffraction and its spin dependence [8].

2. Physics Programme

2.1. Unpolarized Scattering

The QCD proved to be very successful in describing hadronic interactions at large $|t|$ where perturbative methods are applicable. However, for small and medium $|t|$ values in elastic and diffractive scattering, in a the long-range domain, the QCD has not yet provided accurate predictions. This regime of soft hadronic interactions is a field of phenomenological models constrained with asymptotic theorems. The Regge-Gribov theory [3] is based on the analyticity, unitarity and crossing symmetry of the scattering amplitude and describes the interaction via exchange of trajectories related to the poles (or cuts) in the complex angular momentum plane. The elastic channel is treated as a shadow of many inelastic channels. The elastic amplitude is considered to be mainly imaginary and helicity conserving. Phenomenological fits [9, 10, 11, 12] based on Regge theory are able to describe all the hadronic and photoproduction total cross sections in the full energy range. The data are well described by the exchange of the Pomeron (\mathbb{P}) and lower-lying Regge meson, the reggon, trajectories. The Pomeron is described in the QCD language [13] in terms of multi-gluon exchange and point-like coupling to quarks: a color singlet two-gluon exchange with $C = +1$ corresponds to the Pomeron while the color singlet three-gluon $C = -1$ state corresponds to the Odderon [14]. In spite of its successes, the Regge theory still lacks a firm explanation on the QCD grounds. High precision measurements in the energy and $|t|$ -range covered by $\mathcal{P}\mathcal{P}2\mathcal{P}\mathcal{P}$ are certain to have a large impact on this data-driven field.

Figure 1 summarizes present measurements of the total cross section σ_{tot} , the ratio of real to imaginary part of the forward amplitude ρ_0 , and

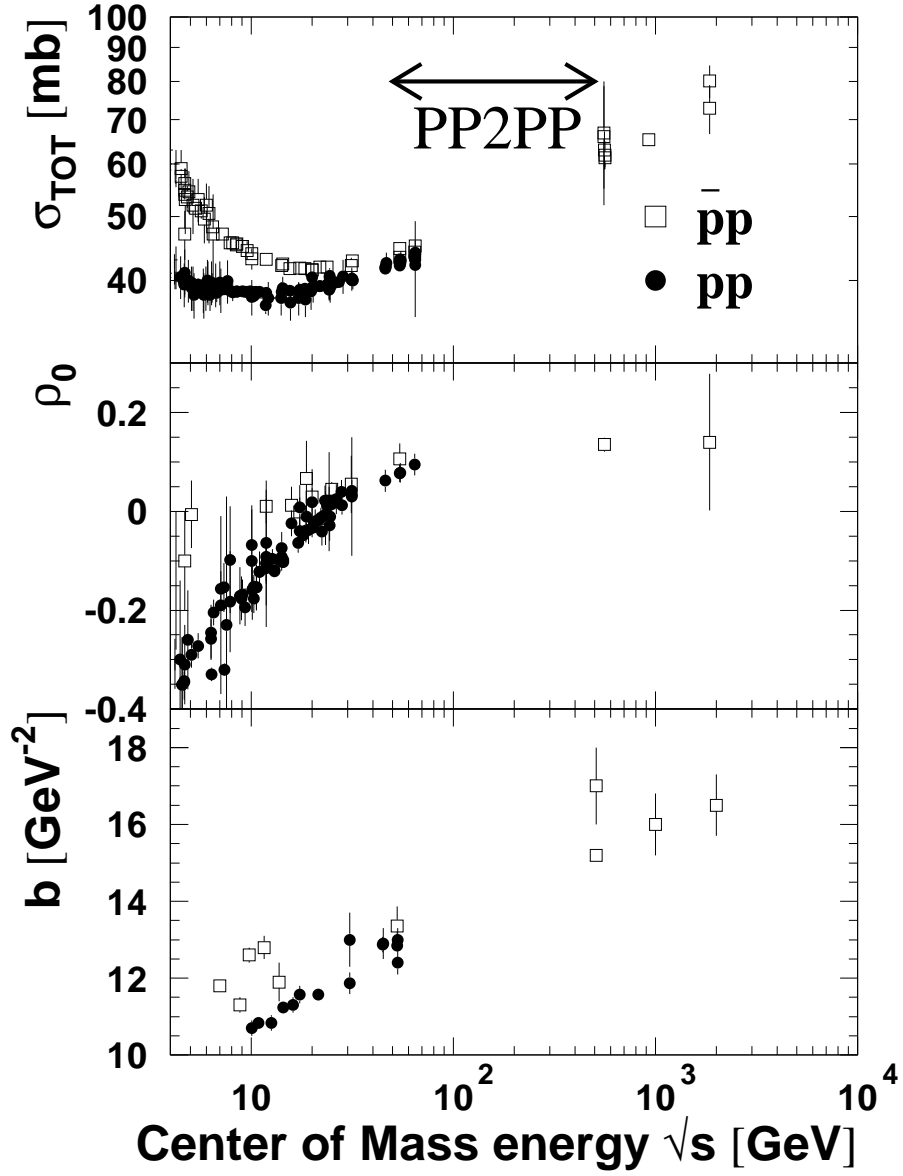


Fig. 1. The total cross section, σ_{tot} , the ρ_0 parameter and the nuclear slope, b , as a function of the centre-of-mass energy.

the nuclear slope b , for both pp and $\bar{p}p$ interactions. The energy range of the $PP2PP$ experiment is also shown. It partially overlaps the high energy ISR region and reaches the low end of the $S\bar{p}pS$ range. A comparison with

existing data at the same energies will be advantageous.

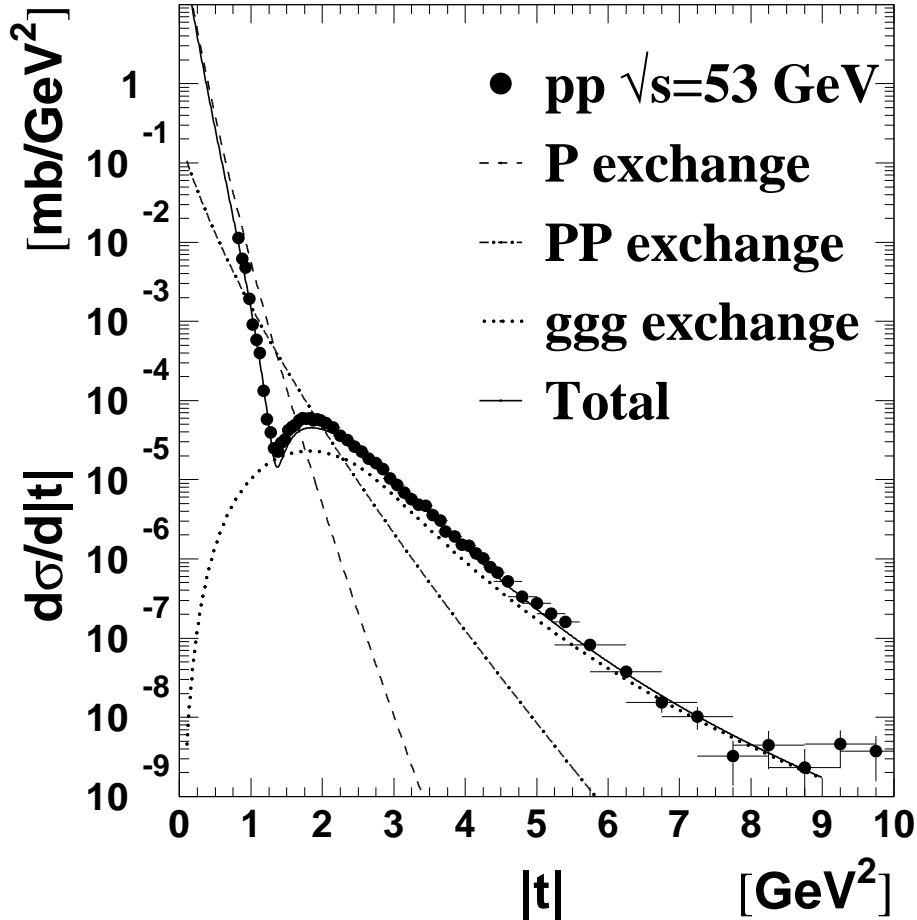


Fig. 2. The differential cross section, in $pp \rightarrow pp$ at $\sqrt{s} = 53$ GeV [15]. The curves are the model [16] predictions.

The differential elastic cross section $d\sigma_{\text{el}}/dt$ as measured at ISR [15] is shown in Fig. 2 together with the phenomenological model [16] predictions. The data show characteristic features: a forward peak followed by an exponential fall, a local minimum above $-t = 1$ GeV² and a secondary maximum or a broad shoulder. The position of the minimum moves toward smaller $|t|$ values with increasing energy. A similar trend is observed for $\bar{p}p$ data. However, the depth of the minimum is smaller than that seen for pp . The data are well described by the model predictions.

The $|t|$ coverage of $\mathcal{PP}2\mathcal{PP}$ includes the “diffraction dip” region. This local minimum was explained [16] by the interference of the exchange ampli-

tudes. In particular, the three-gluon exchange gives a negative contribution in case of pp interaction while for $\bar{p}p$ scattering it is positive.

In the small $|t|$ region the $\mathcal{PP}2\mathcal{PP}$ experiment covers also the Coulomb amplitude dominated domain. Since the Coulomb amplitude is absolutely known then a very small $|t|$ measurement will give an absolute measurement of the accelerator luminosity and an absolute normalization of the hadronic amplitude.

2.2. Polarized Scattering

The understanding of the spin dependence of the scattering amplitudes at high energies and small $|t|$ is very important. It challenges the QCD since it involves its applications in the long-range, non-perturbative regime. New measurements coming from RHIC will test the QCD prediction at a new level of accuracy and detail.

The pp polarization data are commonly discussed using the s-channel helicity amplitudes $\phi_i (i = 1, \dots, 5)$ [17]. Table 1 lists the linear combinations of ϕ_i with definite quantum numbers exchanged asymptotically [18].

Table 1. s-channel amplitudes.

Naturality	Helicity
N_0	$(\phi_1 + \phi_3)/2$
N_1	ϕ_5
N_2	$(\phi_4 - \phi_2)/2$
U_0	$(\phi_1 - \phi_3)/2$
U_1	$(\phi_4 + \phi_2)/2$

The N and U amplitudes correspond to natural and unnatural parity exchange and the subscripts 0, 1 and 2 describe the total s-channel helicity flip involved. The spin-averaged cross sections are given by:

$$\sigma_{\text{tot}} = \frac{1}{K} \text{Im}(N_0(0))$$

and

$$\frac{d\sigma}{dt} = \frac{1}{16\pi K^2} (|N_0|^2 + 2|N_1|^2 + |N_2|^2 + |U_0|^2 + |U_2|^2)$$

where $K = \sqrt{s(s - 4m^2)}$. The most commonly used spin-dependent observables are listed below. The indices stand for different spin orientations: N - along the normal to the scattering plane, S - along the transverse direction in the scattering plane, and L - along the particle direction. The differences of the total cross section for the anti-parallel and parallel spin orientations are

$$\Delta\sigma_N = \sigma^{\uparrow\downarrow} - \sigma^{\uparrow\uparrow} = \frac{1}{K} \text{Im}(N_2(0) - U_2(0))$$

$$\Delta\sigma_L = \frac{1}{K} \text{Im}(U_0(0)).$$

The analysing power, the single-spin asymmetry, is

$$\mathcal{A}_N \frac{d\sigma}{dt} = -2 \frac{1}{16\pi K^2} \text{Im} \{ (N_0 - N_2) N_1^* \},$$

and the double-spin asymmetries are defined as

$$\mathcal{A}_{NN} \frac{d\sigma}{dt} = -2 \frac{1}{16\pi K^2} \left\{ \text{Re}(U_0 U_2^* - N_0 N_2^*) + |N_1|^2 \right\},$$

$$\mathcal{A}_{LL} \frac{d\sigma}{dt} = -2 \frac{1}{16\pi K^2} \left\{ \text{Re}(N_2 U_2^* - N_0 U_0^*) \right\},$$

$$\mathcal{A}_{SS} \frac{d\sigma}{dt} = -2 \frac{1}{16\pi K^2} \left\{ \text{Re}(N_0 U_2^* - N_2 U_0^*) \right\}.$$

To achieve a full amplitude analysis one needs a substantial number of measurements in the same kinematic region. Up till now, the polarization experiments were carried out for \sqrt{s} up to 28 GeV in fixed target environment. This severely affected the minimum values of accessible $|t|$ with exception of the E581/704 Collaboration which used “live-target” to reach down to the CNI region [19]. It is worth pointing out that these problems are non-existing in the RHIC environment since the measurements are performed for protons freely moving in vacuum.

Existing data [20] on the analysing power at $|t| \approx 0.1 - 2.5 \text{ GeV}^2$ show that

- at $|t| < 0.4 \text{ GeV}^2$ \mathcal{A}_N decreases like $1/s$ up to $s \approx 50 \text{ GeV}^2$ and possibly flattens-off around small positive value,
- \mathcal{A}_N becomes negative for $0.4 < |t| < 1 \text{ GeV}^2$ and $s \geq 50 \text{ GeV}^2$, reaches a minimum and again increases crossing zero in the “diffraction dip” region.
- for large $|t|$ the analysing power is constant or possibly decreases to zero above $t \geq 2.5 \text{ GeV}^2$.

The Regge theory predicts [13, 21] that the \mathcal{A}_N should decrease as $s^{-\alpha}$, with $0.5 < \alpha < 1$, since at lower energies hadronic spin-flip amplitude should be dominated by the reggon exchanges. This is confirmed by the data which in the beam momentum range of 45 – 300 GeV/c show very little energy dependence. However, small values of the analysing power can be compatible with zero. On the other hand, the negative values of \mathcal{A}_N for $0.4 < |t| < 1 \text{ GeV}^2$ cannot be deduced from the standard Regge picture.

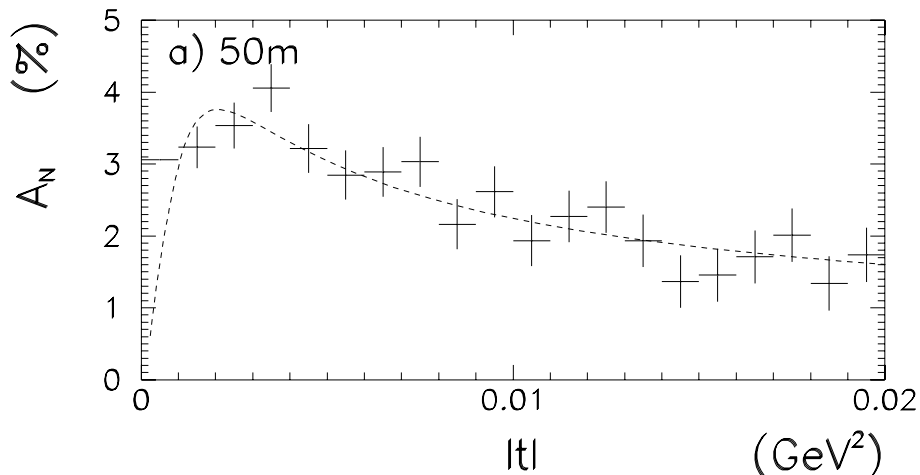


Fig. 3. The theoretical analysing power \mathcal{A}_N (dashed line) superimposed with simulated measurements at $\sqrt{s} = 500$ GeV for stations at 50 m.

A characteristic shape of the $\mathcal{A}_N(t)$ was predicted [22] in the CNI region. The analysing power increases from zero, reaches a maximum at $|t| \approx 0.003$ GeV² and slowly decreases with increasing $|t|$. This structure results from the interference of the electromagnetic spin-flip and hadronic non-flip amplitudes. The maximum \mathcal{A}_N is about 5% and shows a very mild energy dependence. $\mathcal{P}\mathcal{P}2\mathcal{P}\mathcal{P}$, in its first physics run will cover the region around the \mathcal{A}_N maximum and the simulations show that the analysing power can be precisely measured. Figure 3 shows the theoretical predictions [23] with simulated data from the detectors placed 50 meters away from interaction region (IR).

With both RHIC beams polarized, the double spin asymmetry can be measured in a wide $|t|$ range. In the small $|t|$ region it will help to answer the question of the Odderon contribution. A spin-flip amplitude ϕ_5 does not necessarily decrease with increasing energy. This can be due to various mechanisms like peripheral pion production, a di-quark component in the proton, instanton effects or due to the Odderon contribution [24]. In Fig. 4, the theoretical predictions [25] for the Pomeron and Odderon contributions to \mathcal{A}_{NN} are shown. In the higher $|t|$ -region further investigation of experimental observation of large differences for between the cross sections for parallel and anti-parallel spin orientations will be performed. The experiment [26] shows that the protons appear to interact harder when their spins are aligned. However, it is not clear whether this effect is present for higher \sqrt{s} . The measurement of the spin dependent observables in the high- $|t|$ region will reveal the helicity structure of the exchanges. It will address the

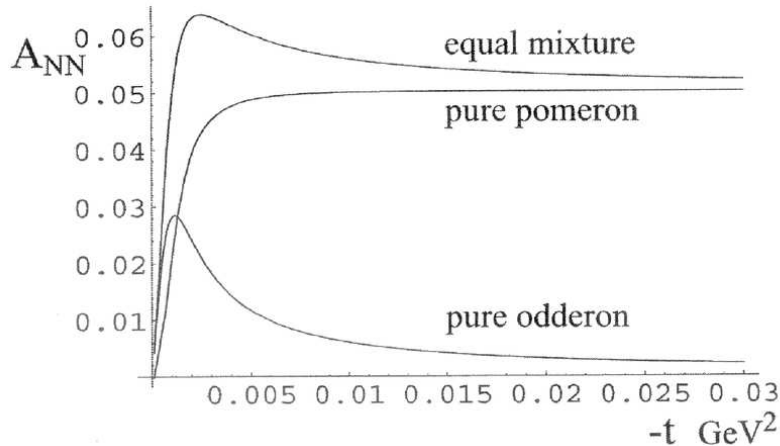


Fig. 4. The Odderon and Pomeron contributions to the double spin asymmetry \mathcal{A}_{NN} from [25].

questions of non-vanishing spin-flip amplitudes in diffraction, the Odderon contribution or whether hard scattering produces large spin effects. They give an insight into the details of the long-range QCD interaction between the protons and possibly how the perturbative regime is approached.

3. The Experimental Setup

The measurement of the small angles observed in elastic scattering requires interfacing of the detectors to the accelerator lattice.

3.1. Method

The proton scattering takes place at the interaction region (IR) at a point (x^*, y^*) , where $x^*(y^*)$ is the horizontal (vertical) coordinate in the plane perpendicular to the accelerator axis. Later the particle traverses inside the beam pipe and is, eventually, registered at (x, y) by the detector. Since the accelerator parameters are known then the scattering angle $-\Theta_y^*$ and the position $-y^*$ at the IR can be calculated from the measured ones. If Ψ denotes the phase advance and β is the betatron function at the detection point then

$$y = \sqrt{\frac{\beta}{\beta^*}} (\cos \Psi + \alpha^* \sin \Psi) y^* + \sqrt{\beta \beta^*} \sin \Psi \Theta_y^*$$

where β^* is the betatron function at the IR, α^* is its derivative and Θ_y^* is the proton scattering angle. For the purpose of this experiment the

machine lattice configurations with $\alpha^* = 0$ were considered. The above formula can be re-written as

$$y = a_{11}y^* + \mathcal{L}_{eff}\Theta_y^* \quad (1)$$

with

$$a_{11} = \sqrt{\frac{\beta}{\beta^*}}(\cos \Psi + \alpha^* \sin \Psi)$$

and

$$\mathcal{L}_{eff} = \sqrt{\beta\beta^*} \sin \Psi.$$

The optimum experimental conditions are for $a_{11} = 0$ ($\alpha^* = 0, \Psi = (2n + 1)\pi/2$) and \mathcal{L}_{eff} as large as possible. Then eq. 1 becomes

$$y = \mathcal{L}_{eff}\Theta_y^*. \quad (2)$$

This means that the scattering angle can be determined from the position measurement alone. In other words the particles scattered at the same angles at the IR will be focused onto the same point. This conditions is known as the “parallel-to-point” focusing.

Another concern for the experimental set-up optimization is the minimum value of the four-momentum transfer $|t|$, namely t_{min} . This value depends on the distance of the detectors to the proton beam. It should be as small as possible to reach the Coulomb dominated region, yet large enough so the machine beams are not destroyed. The value of t_{min} is determined by the minimum scattering angle, Θ_{min} , by

$$t_{min} = (p\Theta_{min})^2,$$

where p is the proton absolute momentum and

$$\Theta_{min} = \frac{d_{min}}{\mathcal{L}_{eff}}, \quad d_{min} = k\sigma_y + d_0$$

where d_{min} is the minimum distance of the approach to the beam, k is the machine dependent factor (10–20) which can be optimized via the beam scraping, σ_y denotes the vertical beam size at the detection point and d_0 measures the detector “dead-space”. If d_0 is small then

$$t_{min} = \frac{\epsilon}{\beta}k^2p^2$$

which means that the the smallest t_{min} can be reached making the betatron function as large as possible and reducing the k-factor and the beam emittance, ϵ .

It is intended to measure the elastic and diffractive scattering for small and medium $|t|$ intervals.

3.2. Layout of the Experiment

Protons scattered at small angles are registered with detectors positioned in the immediate vicinity of the beam. This is achieved with help of a Roman Pot (RP) station [15, 27] placed at the positions for which condition 2 is fulfilled. A layout of the experiment is shown in Fig. 5. In the drawing magnetic elements of the machine lattice (DX , $D0$ and $Q1-Q3$) are shown; symbol $RP1,2$ denotes the Roman Pot station.

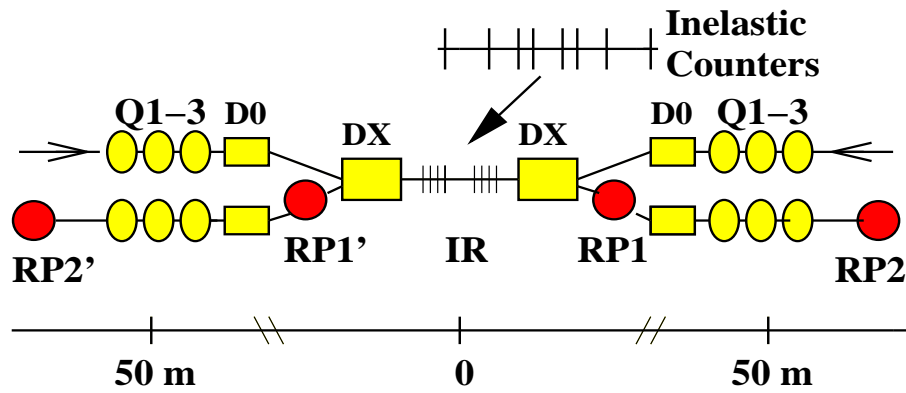


Fig. 5. Layout of the *PP2PP* experiment.

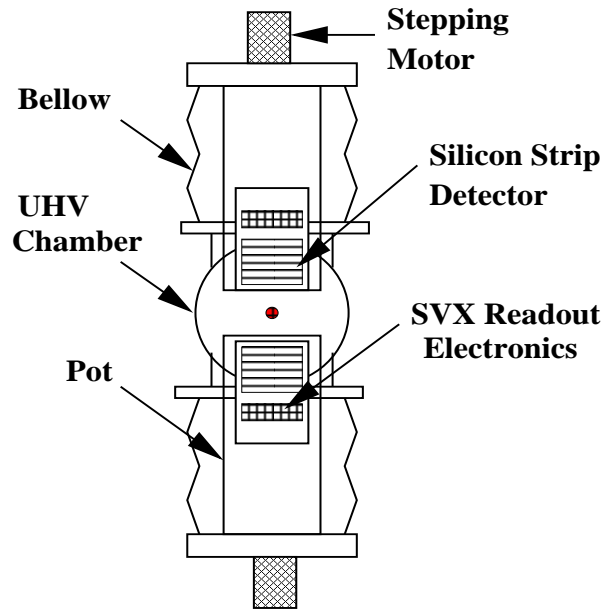


Fig. 6. A schematic view of the Roman Pot station.

The pot, see Fig. 6, allows to insert the detector into the accelerator beam pipe. The active part of the detector consists of four planes of silicon strip detectors out of which two planes measure vertical and two horizontal coordinates. The detectors, 8 by 5 cm², with 100 μ m strip-to-strip and 450 μ m strip-to-edge spacing, are read by the readout system based on the D0 SVX-IIe 128-channel front-end chip and the Stand-Alone Sequencer . This type of detector proved to be a reliable and stable device. It provides:

- a very good uniformity of efficiency,
- small dead area between the detector active part and the beam,
- many highly efficient detector layers,
- small cells,
- good spatial resolution.

3.3. Trigger

There are two basic trigger configurations. The elastic trigger is derived from the scintillator counters placed behind the silicon detectors. The second, inelastic, is used to trigger on diffractive or inelastic events and consists of eight scintillator counters placed symmetrically around the interaction region. The trigger requests a coincidence of the beam crossing and the appropriate scintillators' signals.

3.4. Measurements at Small $|t|$

A special tune of the RHIC accelerator allows reaching the Coulomb region, at $|t|$ values down to 0.0004 GeV². This tune will allow the measurements of very small angles (down to 10 μ rad). Since this tune is not compatible with high luminosity running in other interaction regions it will require a dedicated running period and is postponed beyond 2005. The detector acceptance covers CN region and reaches well into the Coulomb amplitude dominated domain hence it allows for a precise determination of σ_{tot} , ρ_0 and b parameters. To evaluate the detector performance a Monte Carlo was used. Table 2 lists major parameters and their values used in the simulation.

The angular distribution of protons was simulated with small angle CN cross section formula parameterized with σ_{tot} , ρ_0 and b . Using the transport equation the position of the scattered protons at the detector was predicted. Such simulated data were input to the fitting program yielding σ_{tot} , ρ_0 and b . Resulting uncertainties on the parameters are shown as a function of t_{min}

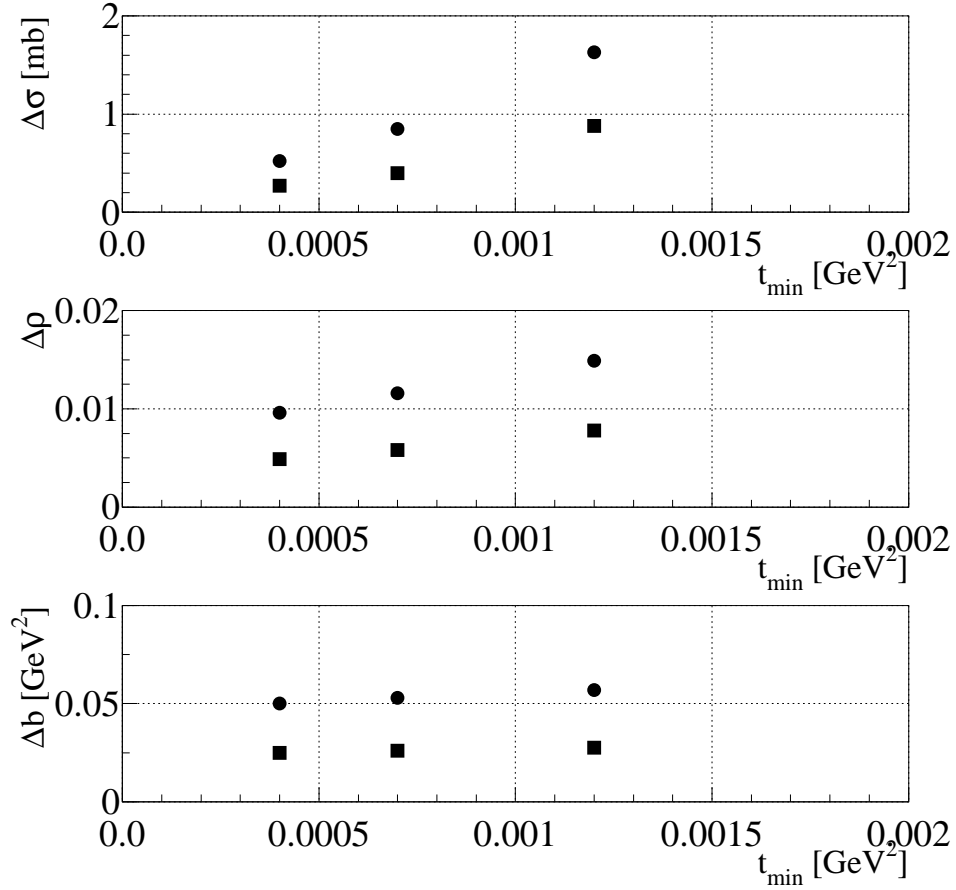


Fig. 7. The uncertainty on the total cross section $\Delta\sigma$, the ratio real to imaginary part of the forward amplitude ρ_0 , and the nuclear slope b as a function of the minimum accessible $|t|$, for 0.8 million events (full dots) and 3.2 million events (full squares) statistics.

in Fig. 7. Two different statistics, $0.8 \cdot 10^6$ and $3.2 \cdot 10^6$, equivalent to one day of stable data taking are compared.

The major contributions to the uncertainties are due to the statistics and the t_{\min} cutoff.

Table 2. Parameters in the Monte Carlo simulation.

Parameter	Value
Beam momentum	250 GeV/c
Beam momentum spread	250 MeV/c
Crossing angle of beams $\Theta_{x,y}^0$	5 μ rad, 5 μ rad
Error on crossing angle $\Delta\Theta_{x,y}^0$	6 μ rad
Detector offsets	20 μ m
Detector resolution in x,y	100 μ m
Interaction region size in z: σ_z	15 cm
Beam emittance: ϵ	5 π mm mrad

3.5. Measurements at Medium $|t|$

The collinearity requirement on the out-going protons will provide identification of the small angle elastic scattering events. Table 3 compares parameters of two earlier [15, 27] and $\mathcal{P}\mathcal{P}2\mathcal{P}\mathcal{P}$ experiments. For the RHIC

Table 3. Parameters of the ISR, UA4 and $\mathcal{P}\mathcal{P}2\mathcal{P}\mathcal{P}$ experiments.

Parameter	ISR	UA4	$\mathcal{P}\mathcal{P}2\mathcal{P}\mathcal{P}$
CMS energy (GeV)	23-62	546-630	50-500
Luminosity $\mathcal{L}(cm^{-2}s^{-1})$	few 10^{30}	few 10^{28}	few 10^{31}
Maximum $ t $ (GeV^2)	10	≈ 2	≈ 1.3
Momentum resolution $\Delta p/p$	$\approx 5\%$	$\approx 0.6\%$	$\approx 1.5\%$
$ t $ resolution Δt	$\approx 0.015\sqrt{ t }$	$\approx 0.06\sqrt{ t }$	$\approx 0.02\sqrt{ t }$

tune $\beta^* = 10$ m, the normalized emittance is $\epsilon = 20\pi$ mm mrad, and at $\sqrt{s} = 500$ GeV the size and the angular spread of the beam at the IR are $\sigma_y = 0.45$ mm and $\sigma_{\Theta_y} = 45$ μ rad, respectively. These parameters were used to calculate the medium- $|t|$ acceptance shown in Fig. 8. The acceptance is larger than 20% for $0.03 \leq |t| \leq 1.3$ GeV^2 . This is the interval which covers the “diffractive dip” region at $\sqrt{s} = 500$ GeV. At larger $|t|$ values the acceptance is limited due to the DX magnet’s aperture cut at 5.4 mrad. At $|t| = 1$ GeV^2 , the expected cross section is 0.001 mb/ GeV^2 . The detector acceptance is about 35%. At RHIC luminosity $\mathcal{L} = 10^{31}cm^{-2}s^{-1}$ about 10^4 elastic events per $|t|$ -bin of 0.05 GeV^2 per day is expected which shows that running time is not a limitation.

4. Running Plan

The data collection will be staged due to the experimental setup staging and the accelerator operation mode requirements.

Acceptance for medium t

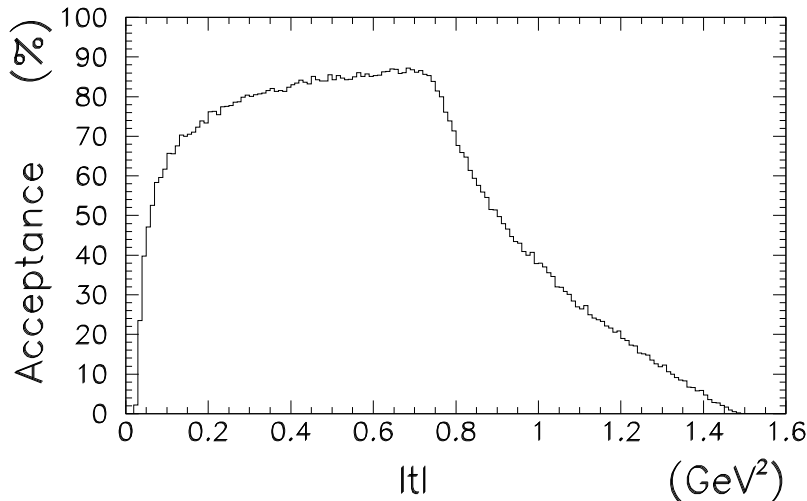


Fig. 8. The medium- $|t|$ acceptance of the detectors.

In 2002, the experimental apparatus will consist of the two fully equipped stations. These stations will be placed in the RHIC tunnel about 57 meters away from the interaction region. In January, it is planned to collect the data at $\sqrt{s} = 200$ GeV. The accelerator will operate with $\beta^* = 10$ m. The useful range of the four-momentum transfer will be: $0.004 \leq -t \leq 0.02$ GeV². With collected data it will be possible to measure the nuclear slope parameter and possibly the single spin asymmetry \mathcal{A}_N .

In 2003, there will be four fully equipped stations used for the data taking. It is planned to run at $\sqrt{s} = 200$ GeV for $0.0004 \leq -t \leq 0.02$ GeV². This run will be devoted to the study of the CNI region and the energy dependence of σ_{tot} , ρ , b and spin asymmetries: \mathcal{A}_N , \mathcal{A}_{NN} . About one day of stable running is necessary to obtain the error on analysing power of $\Delta A_N \approx 0.2 - 0.3\%$ for A_N value $\approx 4\%$.

For 2004, a major update of the experimental setup is foreseen. Additional Roman Pot stations will be placed in the straight sections connecting the DX and $D0$ magnets, see Fig. 5. This will enable the measurements for $-t \leq 1.3$ GeV². The energy dependence of the nuclear slope, elastic differential cross section and spin observables will be investigated. Also the diffractive minimum region will be studied. At luminosity $\mathcal{L} = 4 \cdot 10^{30} \text{ cm}^{-2} \text{ s}^{-1}$

about 200 hours of the data taking will be needed to acquire 1000 events per 0.02 GeV^2 bin around $-t = 1 \text{ GeV}^2$.

Investigation of the very small $|t|$ region will require a special, $\mathcal{PP}2\mathcal{PP}$ dedicated tune of the accelerator, $\beta^* \approx 100\text{m}$. Therefore precision measurements of ratio of the real-to-imaginary part of the forward amplitude, of the total cross section for $0.0004 \leq -t \leq 0.12 \text{ GeV}^2$ will be postponed until after 2004.

It is worth noting that the same experimental setup can be used to measure the elastic scattering of pd , $p^\uparrow d$, dd and $p^\uparrow {}^4\text{He}$. It is also possible to extend the four-momentum region beyond 1.3 GeV^2 by adding RP stations in front of the DX magnets.

5. Summary

The $\mathcal{PP}2\mathcal{PP}$ experiment at RHIC Collider has been introduced. The physics programme includes a systematic study of the spin dependent and spin independent features of the elastic proton – proton scattering in wide and mostly unexplored energy domain $50 \leq \sqrt{s} \leq 500 \text{ GeV}$ and for the four-momentum transfer $0.0004 \leq |t| \leq 1.3 \text{ GeV}^2$ within a single experiment. The use of the same apparatus will play a crucial role in understanding and reduction of systematic errors. Elastically scattered protons will be measured with silicon detectors placed in the Roman Pots. New and precise measurements coming from the $\mathcal{PP}2\mathcal{PP}$ experiment will help to test the QCD in a non-perturbative regime. They will also shed light on the helicity structure of the proton and that of the object exchanged in the interaction.

REFERENCES

- [1] S. Bültmann, I. H. Chiang, B. Chrien, A. Drees, R. Gill, W. Guryn, D. Lynn, P. Pile, A. Rusek, M. Sakitt, S. Tepikian, Brookhaven National Laboratory, USA, J. Chwastowski, B. Pawlik, Institute of Nuclear Physics, Cracow, Poland, J. Bourotte, M. Haguenaue, Ecole Polytechnique/IN2P3-CNRS, Palaiseau, France, N. Akchurin, C. Newsom, Y. Onel, University of Iowa, Iowa City, USA, A. A. Bogdanov, V. A. Kaplin, A. Karakash, S.B. Nurushev, M.F Runtzo, M. N. Strikhanov, Moscow Engineering Physics Institute (MEPHI), Moscow, Russia, A. Ufimtsev, IHEP Serpukhov, Russia, I. G. Alexeyev, V. P. Kanavets, B. V. Morozov, D. N. Svirida, ITEP, Moscow, Russia, M. Rijssenbeek, C. Tang, S. Yeung, SUNY Stony Brook, USA, K. De, N. Guler, A. Vartapetian, University of Texas at Arlington, USA, R. Giacomich, A. Penzo, P. Schiavon, Universita di Trieste and Sezione INFN, Italy, A. Sandacz, Institute for Nuclear Studies, Warsaw, Poland
- [2] W. Heisenberg, *Z. Phys.* **133** (1952) 65.

- [3] See e.g. P. D B. Collins, “An Introduction to Regge Theory and High Energy Physics’ Cambridge UP, Cambridge 1977,
P. D B. Collins and A. Martin, “Hadron Interactions” Adam Hilger 1984, and references therein.
- [4] I. Y. Pomeranchuk, *Sov. Phys. – JETP***7** (1958) 499.
- [5] G. Mattie, *Proc. Proton and Antiproton Cross Sections at High Energies, Rep. Prog. Phys.* **57** (1994) 743,
A. Martin, *Proc.of International Conf. on Elastic and Diffractive Scattering*, eds. M. M. Bock and A. R. White (1989),
F. Halzen, Summary Talk Blois V, *Proc.of International Conf. on Elastic and Diffractive Scattering* eds. H. M. Fried, K. Kang, C-I. Tan, Providence (1993), World Scientific 1994
M. Allbrow, Experimental Summary Talk Blois V, *Proc.of International Conf. on Elastic and Diffractive Scattering* eds. H. M. Fried, K. Kang, C-I. Tan, Providence (1993), World Scientific 1994,
M. Block, *Proc.of International Conf. on Elastic and Diffractive Scattering*, eds. H. M. Fried, K. Kang, C-I. Tan, Providence (1993), World Scientific 1994.
- [6] G. Bunce, “RHIC Polarized Proton Collider: Plans and Schedule”, Published in “Hamburg/Zeuthen 1997, Deep inelastic scattering off polarized targets, Physics with polarized protons at HERA” 466-471.
- [7] W. Guryn *et al.*, “ $\mathcal{PP}2\mathcal{PP}$ Proposal to Measure Total and Elastic pp Cross Sections at RHIC” (unpublished).
- [8] N. H. Buttimore, B. Z. Kopeliovich, E. Leader, J. Soffer, T. L. Truemann, *Phys. Rev.* **D59** (1999) 114010.
- [9] A. Donnachie and P.V. Landshoff, *Phys. Lett.* **B296** (1992) 227.
- [10] J.R. Cudell *et al.*, *Phys. Rev.* **D61** (2000) 034019,
Erratum-*Phys. Rev.* **D63** (2001) 059901.
- [11] A. Donnachie and P.V. Landshoff, *Phys. Lett.* **B437** (1998) 408.
- [12] M.M. Block *et al.*, *Phys. Rev.* **D60** (1999) 054024,
M.M. Block, F. Halzen and T. Stanev, *Phys. Rev.* **D62** (2000) 077501.
- [13] F. E. Low *Phys. Rev.* **D12** (1975) 163,
S. Nussimov *Phys. Rev. Lett.* **34** (1975) 1268,
L. N. Lipatov *Nucl. Phys.* **B365** (1991) 641.
- [14] P. Gauron, E. Leader and B. Nicolescu, *Nucl. Phys.* **B299** (1985) 640.
- [15] E. Nagy *et al.*, *Nucl. Phys.* **B150** (1979) 221.
- [16] A. Donnachie and P.V. Landshoff, *Nucl. Phys.* **B231** (1984) 189.
- [17] M. Jacob and G. C. Wick, *Ann. Phys.* **7** (1959) 404,
M. L. Goldberger, M. T. Gisar, S. MacDowell, D. Y. Wang, *Phys. Rev.* **120** (1960) 2250.
- [18] E. L. Berger, A. C. Irving and C. Sorensen, *Phys. Rev.* **D17** (1978) 2971.
- [19] N. Akchurin *et al.*, *Phys. Lett.* **B29** (1989) 299,
Phys. Rev. **D48** (1993) 3026.

- [20] M. Borghini *et al.*, *Phys. Lett.* **B31** (1970) 405, *Phys. Lett.* **B36** (1971) 501, G. W. Abshire *et al.*, *Phys. Rev. Lett.* **32** (1974) 1261, A. Gaidot *et al.*, *Phys. Lett.* **B61** (1976) 103, D. G. Crabb *et al.*, *Nucl. Phys.* **B121** (1977) 231, J. Antille *et al.*, *Nucl. Phys.* **B185** (1981) 1, D. G. Crabb *et al.*, *Phys. Rev. Lett.* **65** (1990) 3421, G. Fidencaro *et al.*, *Phys. Lett.* **B76** (1978) 369, *Phys. Lett.* **B105** (1981) 309, *Nucl. Phys.* **B173** (1980) 513, J. H. Snyder *et al.*, *Phys. Rev. Lett.* **41** (1978) 781, M. Corcoran *et al.*, *Phys. Rev.* **D22** (1980) 2624, R. V. Kline *et al.*, *Phys. Rev.* **D22** (1980) 553.
- [21] For example (see also references therein): G. C. Fox and C. Quigg, *Ann. Rev. Nucl. Sci.* **23** (1973) 219, F. Halzen and G. Thomas, *Phys. Rev.* **D10** (1977) 344, A. McNeil and S. J. Wallace, *Phys. Rev.* **D21** (1980) 1434, G. L. Kane and A. Seidl, *Rev. Mod. Phys.* **48** (1976) 309, H. P. Gerhold and W. Majerotto, *Nuovo Cimento Lett.* **23** (1978) 281, S. M. Troshin and N. E. Tyurin, *Phys. Lett.* **144B** (1984) 260.
- [22] J. Schwinger, *Phys. Rev.* **69** (1946) 481, *Phys. Rev.* **73** (1948) 407, B. Z. Kopeliovich and L. I. Lapidus, *Sov. J. Nucl. Phys.* **19** (1974) 114, N. H. Buttimore, E. Gotsman and E. Leader, *Phys. Rev.* **18** (1978) 694, C. Bourrely and J. Soffer, *Nuovo Cimento Lett.* **19** (1977) 569, R. Jakob and P. Kroll, *Z. Phys.* **A344** (1992) 87, O. V. Selyugin, *Int. J. Mod. Phys.* **A12** (1997) 1379.
- [23] N. Akchurin *et al.*, “Polarimetry for High Energy Polarized Proton Colliders with a Jet Target”, Proc. 12th Int. Symp. on High-Energy SpinPhysics, Sept. 1996, Amsterdam. eds. C. W. de Jager *et al.*, (1987) 810, Publ. World Scientific.
- [24] G. L. Kane and J. Pumplin, *Phys. Rev.* **D11** (1975) 1183, K. Hinotani *et al.*, *Nuovo Cimento* **A52** (1979) 363, M. Kamran, *J. Phys.* **G8** (1982) 33, B. Z. Kopeliovich and B. C. Zakharov, *Phys. Lett.* **B226** (1989) 156, S. V. Goloskov, *Phys. Lett.* **B315** (1993) 459, M. Anselmino and S. Forte, *Phys. Rev. Lett.* **71** (1993) 223, see also [25].
- [25] E. Leader and T.L. Trueman, *Phys. Rev.* **D61** (2000) 077504.
- [26] D. G. Crabb *et al.*, *Phys. Rev. Lett.* **41** (1978) 1257, E. A. Crosbie *et al.*, *Phys. Rev.* **D23** (1981) 600.
- [27] M. Bozzo *et al.*, *Phys. Lett.* **B155** (1985) 197, R. Batisson *et al.*, *Nucl. Instr. and Meth.* **A238** (1985) 35.